Tunable Band Gap of MoS_2/BN van der Waals Heterostructures under an External Electric Field

M. Luo[a,*], B. Yu[a] and Y.H. Shen[b]

[a]Department of Physics, Shanghai Polytechnic University,
No. 2360, Jinhai Road, Pudong New District, Shanghai 201209, China

[b]Key Laboratory of Polar Materials and Devices, East China Normal University, Shanghai 200241, China

(Received February 25, 2018; in final form January 28, 2019)

The density functional theory calculations are performed on the structural and electronic properties of the MoS_2/BN van der Waals heterostructure under an external electric field (E-field). Our results reveal that the MoS_2/BN van der Waals heterostructure has a direct band gap of 1.81 eV in the raw, and electrons prefer to transfer from MoS_2 to BN due to the deeper potential of BN monolayer. Moreover, by applying an E-field, ranging from –0.40 to +0.50 V/Å, the band gap decreases from 1.81 eV to zero, which is linked to the direction and strength of the E-field. Through partial density of states plots, it is revealed that d and p orbitals of Mo, S, B, and N atoms are responsible for the significant variations of the band gap. These obtained results predict that the tunable band gap of the MoS_2/BN van der Waals heterostructure carries potential applications for nanoelectronic and spintronic devices.

DOI: 10.12693/APhysPolA.135.391
PACS/topics: 68.65.Ac, 73.20.At, 74.20.Pq

1. Introduction

Graphene, as a typical monolayer honeycomb structure, has got wide interest. A large number of researches have verified its superior properties than conventional materials [1–3]. Two-dimensional (2D) materials will have potential applications for future nanoscale devices [4, 5]. However, the 2D materials still face important challenges, such as growth of large areas, the integration in current Si-based nanotechnologies, which seriously restricts its practical application. In this aspect, searching substitutable 2D materials, which have supereminent chemical and physical properties, is under significant research interests [6–9]. Among those 2D materials, MoS_2 and BN monolayers have been widely studied [10–14], which give useful information to produce potential applications in electronic and optoelectronic devices.

Discovery of new 2D materials, has stimulated the scientific community to study and analyze the van der Waals (vdW) heterostructures, which consisted of different types of different 2D materials. It has been suggested in previous studies that the vdW hetero-structures having unique chemical and electronic properties, such as graphene/BN [15, 16], graphene/TMD [17, 18], phosphorene/TMD [19], hold wide range of technological applications. In order to facilitate the vdW heterostructures to be utilized for spintronic device applications, it is crucial to modulate the band gap with the help of geometrical strain or an external electric field (E-field) [20–25]. Monolayer MoS_2 and h-BN contain similar atomic structures; it is worthwhile to investigate the MoS_2/BN vdW heterostructures and unique electronic properties different form pristine MoS_2 and BN would be expected.

In this study, we try to investigate electronic structures of the MoS_2/BN vdW heterostructures under the application of an external E-field. First-principles calculations have been performed on the MoS_2/BN vdW heterostructures and aforementioned properties have been investigated comprehensively. Without any E-field, a direct band gap of 1.81 eV is shown. With an external E-field, very interesting phenomena have been observed. A tunable band gap, ranging from 0 to 1.81 eV, has been observed and the decreasing tendency is related to the direction and the strength of E-field. Our obtained results can enable the electronic properties of the MoS_2/BN vdW heterostructure to be modified for desired engineering applications, particularly spintronic and nanoelectronics device applications.

2. Calculation details

The electronic and magnetic properties in this paper are performed by the DFT implemented in the VASP code [26]. The Perdew–Burke–Ernzerhof (PBE) of exchange-correlation calculations with the generalized gradient approximation (GGA) are used [27]. The projector-augmented wave (PAW) potentials [28] are used with a 450 eV cut-off energy. The vdW correction (DFT-D2) within the PBE functional proposed by Grimme is applied [29]. A set of $5 \times 5 \times 1$ k-points are used. The lattice constants of 2D-BN and 2D-MoS_2 are 2.503 and 3.160 Å. The MoS_2/BN vdW heterostructure is made up of a $4 \times 4 \times 1$ MoS_2 monolayer and a $5 \times 5 \times 1$ BN monolayer, as shown in Fig. 1a and b. The MoS_2/BN

*corresponding author; e-mail: luomin@sspu.edu.cn

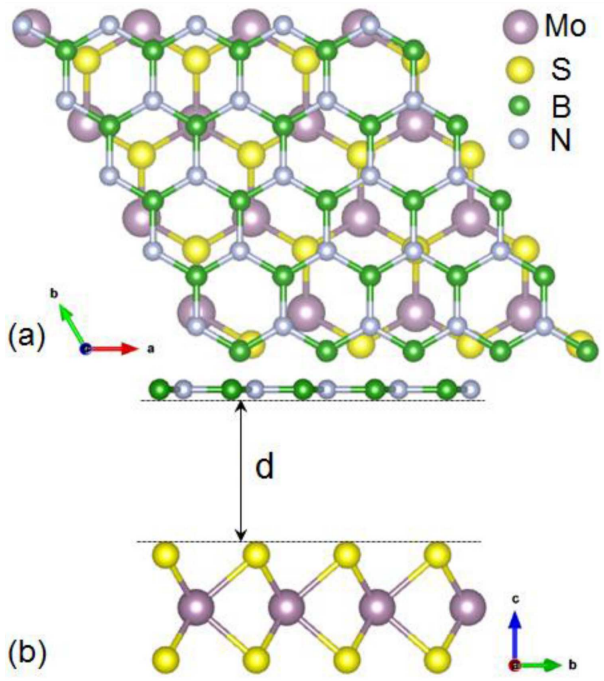

Fig. 1. (a) Top and (b) side views of the MoS_2/BN vdW heterostructure. The interlayer distance d changes along the c-axis.

vdW heterostructure possessing only 1.2% lattice disparity, has little effects on the electronic properties in the vdW heterostructure. To simulate the MoS_2/BN vdW heterostructure, a vacuum of 20 Å along the z-direction is added. Geometry relaxation was processed until, the given structures were fully optimized, and the Hellmann–Feynman forces less than 0.01 eV/Å and the total change in energy less than 10^{-6} eV was obtained.

3. Results and discussion

Firstly, we explored the electronic structure of pristine BN and MoS_2 monolayer. The BN and MoS_2 monolayers have direct band gaps of 4.50 and 1.79 eV, as shown in Fig. 2a and b. These results are consistent with previous studies [11, 30], which verifies the reliability of our methods. We calculated the binding energy for the MoS_2/BN bilayer in order to verify the stability of given systems using the following expression:

$$E_b = E_T - (E_{\mathrm{MoS_2}} + E_{BN}),$$

where E_T is the total energy of the MoS_2/BN vdW heterostructure; E_{MoS2} and E_{BN} are the total energies of pure MoS_2 and BN monolayers. Based on calculated binding energies, as shown in Fig. 3, the binding energy changes demanding on the distance between MoS_2 and BN monolayers and gets the lowest value of –0.093 eV at an equilibrium distance of $d_0 = 4.80$ Å. Moreover, we calculate the plane averaged charge density differences and electrostatic potentials of the vdW heterostructure with different interlayer distances, respectively. As shown

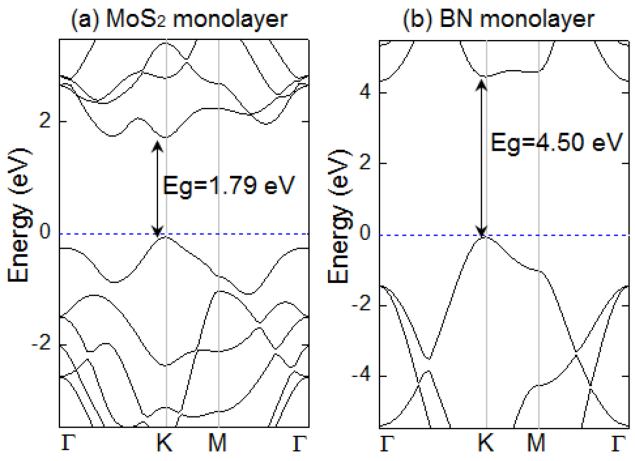

Fig. 2. Band structures of pristine (a) MoS_2 monolayer and (b) BN monolayer. The Fermi level is marked by the dashed line.

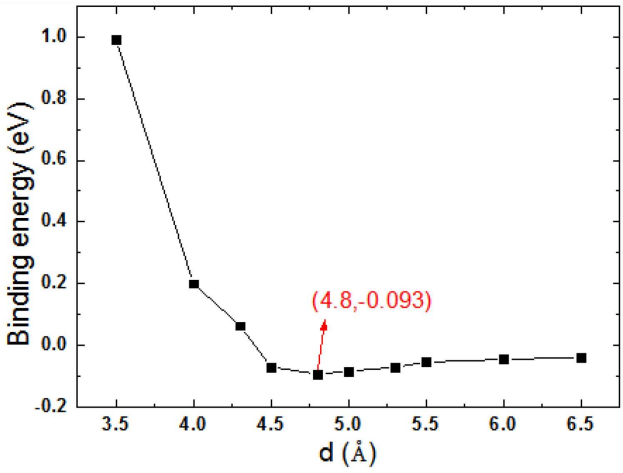

Fig. 3. Binding energy of the MoS_2/BN bilayer as a function of the interlayer distance.

in Fig. 4a, the BN monolayer has a deeper electrostatic potential than the MoS_2 monolayer. It is obvious that electrons could be easily transferred from MoS_2 to BN monolayer. Our results verified that as the interlayer distances decrease, more electrons are transferred from the MoS_2 to the BN layer, as shown in Fig. 4b.

It is noteworthy that the band gap of the MoS_2/BN vdW heterostructure seems to remain unchanged, as shown in Fig. 5a and b. A value of 1.81 eV is observed at the equilibrium distance. Next, we study the electronic properties of the MoS_2/BN vdW heterostructures by applying an external E-field. The band gaps under different strength of the E-field ($\mathcal{E}$) are described in Fig. 6. There are two directions of E-field along the z-axis. The negative direction ($-\mathcal{E}$) is defined as the direction from top to bottom of the vdW heterostructures, and the positive direction ($+\mathcal{E}$) is its reversed direction. In our calculations, the E-field, ranging from −0.50 to +0.60 V/Å, is not likely to change structural properties, but just causes

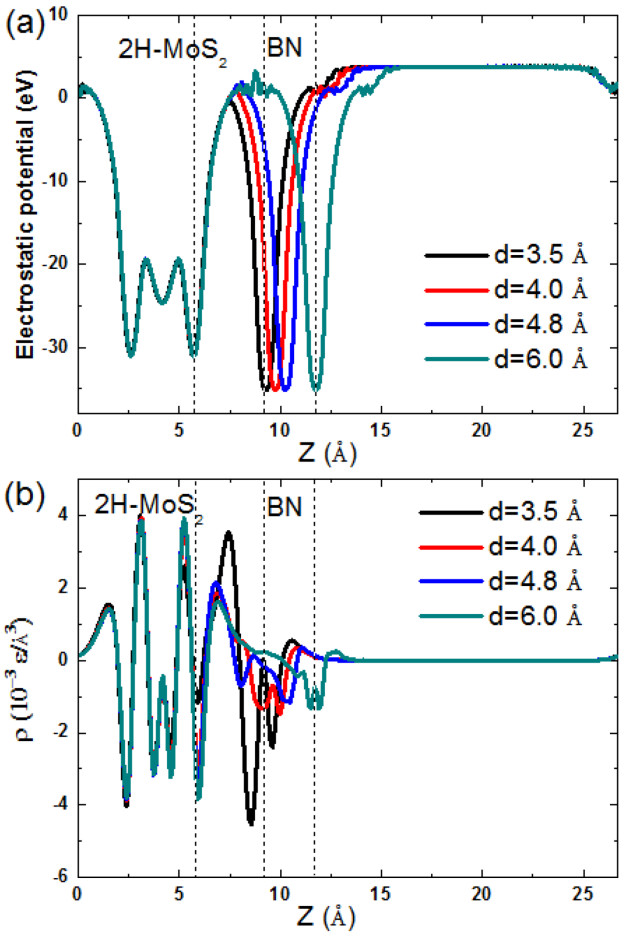

Fig. 4. (a) Electrostatic potentials and (b) plane-averaged charge density differences of the MoS_2/BN vdW heterostructure with different interlayer distances.

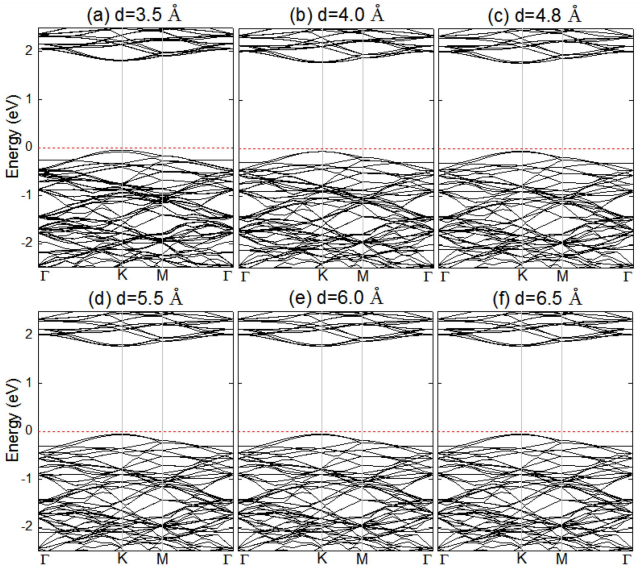

Fig. 5. Band structures of the MoS_2/BN vdW heterostructure with different interlayer distances. The Fermi levels are marked by the red dashed line.

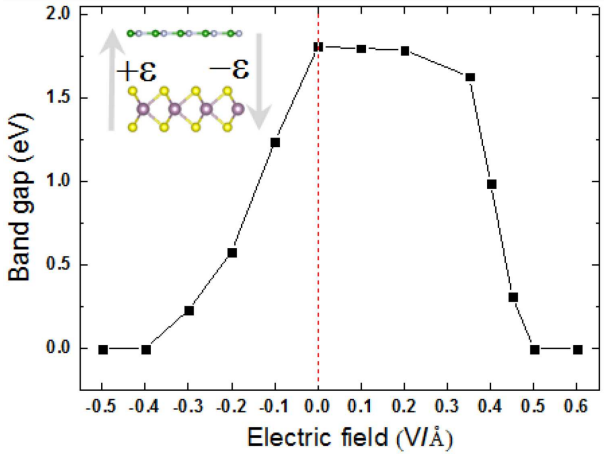

Fig. 6. Band gap of the MoS_2/BN vdW heterostructure as a function of the external electric field.

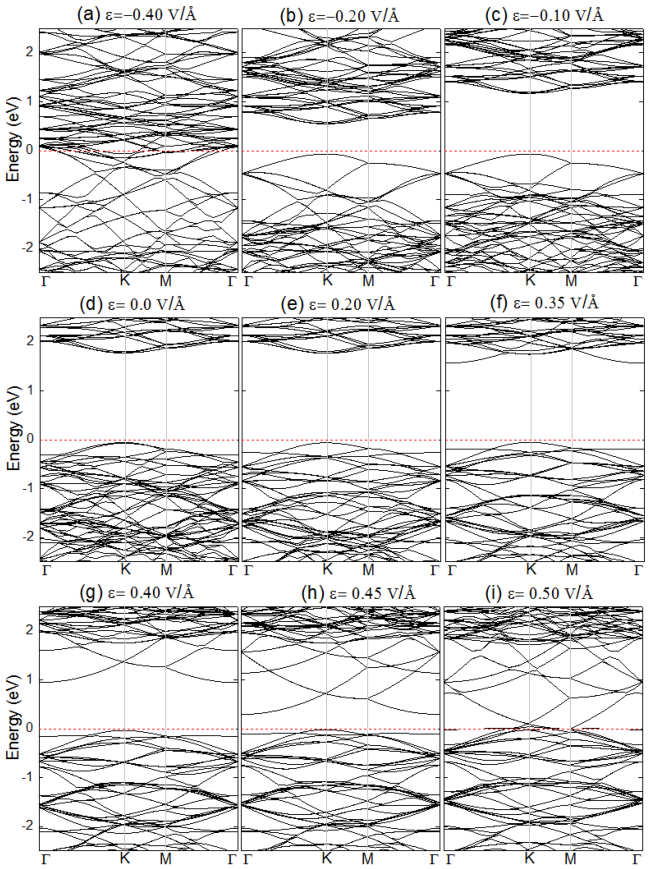

Fig. 7. Band structures of the MoS_2/BN vdW heterostructure with different E-field strength. The Fermi levels are marked by the red dashed line.

redistribution of charges [31, 32]. It is observed that both the strength and direction of E-field have effects on the variations of the band gap. The MoS_2/BN bilayer exhibits roughly parabolic relationship between the band gap and the E-field as the $\mathcal{E}$ changes from -0.50 to $+0.60$ V/Å. While the $-\mathcal{E}$ is applied, the band gap gradually decreases from 1.81 to 0 eV and the band gap

disappears at −0.40 V/Å. Different behavior shows while the $+\mathcal{E}$ is applied. The band gap keeps the same (≈ 1.81 eV) at the range of 0 to +0.20 eV, and then decreases to zero fast. Moreover, it seems that the direction of the E-field has some effects on the band gap, and the $-\mathcal{E}$ has much more influence on the band gap in current system.

Band structures under different E-field are presented in Fig. 7. Some changes happen in both the conduction band minimum (CBM) and the valence band maximum (VBM). As shown in Fig. 7a–d, under the $-\mathcal{E}$, on the one hand part of the VBM moves far away from the Fermi level (E_F) but the top of the VBM stays the same. On the other hand, the whole CBM shifts to the E_F as the E-field strength enhances, then the band gap reduces and eventually disappears. In contrast, under the $+\mathcal{E}$, quite different phenomenon appears. As shown in Fig. 7e–i, the whole VBM seems to be unchanged as the E-field increases, but part of the CBM shifts to the E_F, which attributes to modification of the band gap. To analyze the variation of band gap, the partial density of states (PDOS) are presented in Fig. 8. Obtained results indicate that different states of Mo, S, B, and N atoms are mainly responsible for the significant variations of band gaps. As provided in Fig. 8a and b, under the negative E-field, the states at the top of the valence band are mainly due to the d-orbital of Mo and partly due to the p-orbital of S, and states at bottom of the conduction band are owed to the p-orbital of N. Under the positive E-field, as shown in Fig. 8d and e, the p-orbital of B contributes to the modification of CBM, which crucially induces the increase of variations in the band gap. By contrast, the states at the top of the valence band are due to both the p-orbital of S and the d-orbital of Mo.

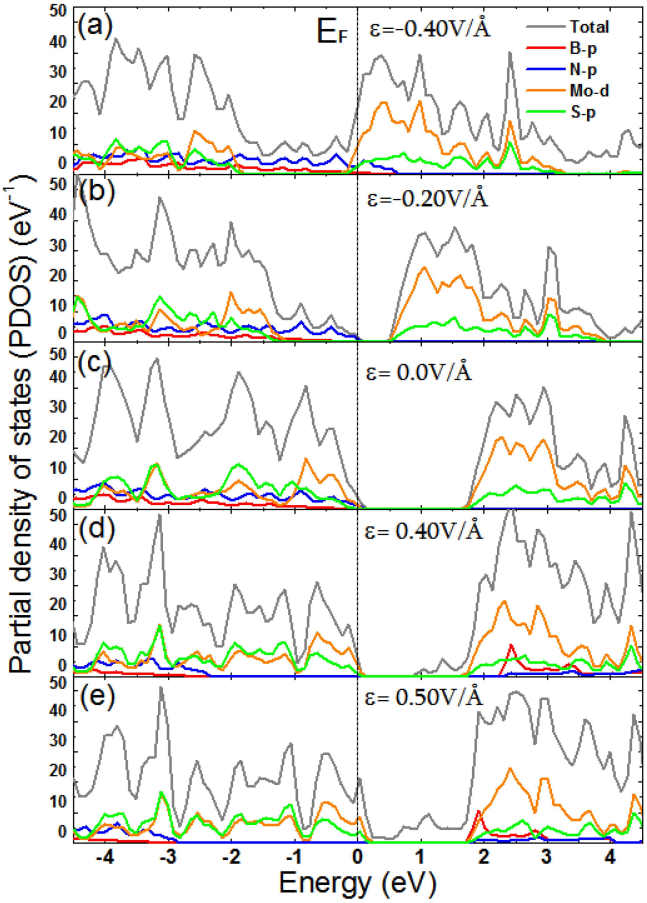

Fig. 8. PDOS of the MoS_2/BN vdW heterostructure with different E-field strength. The Fermi level is marked by the black dashed line.

4. Conclusions

In this study, we systematically investigated the effects of E-field on the electronic properties of the MoS_2/BN vdW heterostructure by using the first-principles calculations. The system showed a direct band gap of 1.81 eV at the equilibrium state. The results of charge density differences and electrostatic potential implied that more electrons were likely to transfer from MoS_2 to BN monolayer. It was revealed that the band gap of the vdW heterostructure are highly sensitive to the E-field. As the E-field changed in the range of −0.50 to +0.60 V/Å, the band gap decreased and approximately showed a parabola-like relation around 0 V/Å. Based on the analysis of band structures and PDOS, such significant variations of band gap are induced by different states of Mo, S, B, and N atoms. Our results might be helpful for experimental extrapolation, thus introducing the MoS_2/BN vdW heterostructure into spintronic and optoelectronic device applications.

Acknowledgments

The work is supported by the Discipline Project of Shanghai Polytechnic University (grant No. XXKZD1605), the Foundation of Shanghai Polytechnic University (grant No. EGD18XQD29), the Shanghai Committee of Science and Technology, China (grant No. 13YZ133), and the National Natural Science Foundation of China (grant No. 51776116). Our work is also supported by the Research Center of Resource Recycling Science and Engineering, Shanghai Polytechnic University, and Gaoyuan Discipline of Shanghai-Environmental Science and Engineering (Resource Recycling Science and Engineering).

References

[1] K.S. Novoselov, A.K. Geim, S.V. Morozov, D. Jiang, Y. Zhang, S.V. Dubonos, I.V. Grigorieva, A.A. Firsov, *Science* **306**, 666 (2004).

[2] A.K. Geim, K.S. Novoselov, *Nat. Mater.* **6**, 183 (2007).

[3] A.H. Castro Neto, F. Guinea, N.M.R. Peres, K.S. Novoselov, A.K. Geim, *Rev. Mod. Phys.* **81**, 109 (2009).

[4] K.F. Mak, C. Lee, J. Hone, J. Shan, T.F. Heinz, *Phys. Rev. Lett.* **105**, 136805 (2010).

[5] B. Radisavljevic, A. Radenovic, J. Brivio, V. Giacometti, A. Kis, *Nat. Nanotechnol.* **6**, 147 (2011).

[6] A.S. Rodin, A. Carvalho, A.H. Castro Neto, *Phys. Rev. Lett.* **112**, 176801 (2014).

[7] T. Low, A.S. Rodin, A. Carvalho, Y. Jiang, H. Wang, F. Xia, A.H. Castro Neto, *Phys. Rev. B* **90**, 075434 (2014).

[8] R. Fei, A. Faghaninia, R. Soklaski, J.A. Yan, C. Lo, L. Yang, *Nano Lett.* **14**, 6393 (2014).

[9] A. Ramasubramaniam, A.R. Muniz, *Phys. Rev. B* **90**, 085424 (2014).

[10] M. Xu, T. Liang, M. Shi, H. Chen, *Chem. Rev.* **113**, 3766 (2013).

[11] B. Huang, H. Lee, *Phys. Rev. B* **86**, 245406 (2012).

[12] Y. Lin, J.W. Connell, *Nanoscale* **4**, 6908 (2012).

[13] J. Qi, X. Li, X. Qian, J. Feng, *Appl. Phys. Lett.* **102**, 173112 (2013).

[14] Q.H. Wang, K. Kalantar-Zadeh, A. Kis, J.N. Coleman, M.S. Strano, *Nat. Nanotechnol.* **7**, 699 (2012).

[15] A. Woessner, M.B. Lundeberg, Y. Gao, A. Principi, P. Alonso-Gonzalez, M. Carrega, K. Watanabe, T. Taniguchi, G. Vignale, M. Polini, J. Hone, R. Hillenbrand, F.H.L. Koppens, *Nat. Mater.* **14**, 421 (2015).

[16] C.H. Zhang, C.H. Jin, A.L. Koh, Y. Zhou, W.G. Xu, Q.C. Li, Q.H. Xiong, H.L. Peng, Z.F. Liu, *Nat. Commun.* **6**, 6519 (2015).

[17] H.C. Diaz, J. Avila, C.Y. Chen, R. Addou, M.C. Asensio, M. Batzill, *Nano Lett.* **15**, 1135 (2015).

[18] M. Yankowitz, S. Larentis, K. Kim, J. Xue, D. McKenzie, S. Huang, M. Paggen, M.N. Ali, R.J. Cava, E. Tutuc, B.J. LeRoy, *Nano Lett.* **15**, 1925 (2015).

[19] Y.X. Deng, Z. Luo, N.J. Conrad, H. Liu, Y.J. Gong, S. Najmaei, P.M. Ajayan, J. Lou, X.F. Xu, P.D. Ye, *ACS Nano* **8**, 8292 (2014).

[20] V.M. Pereira, A.H.C. Neto, *Phys. Rev. Lett.* **103**, 046801 (2009).

[21] J.D. Zhu, J.C. Zhang, Y. Hao, *Jpn. J. Appl. Phys.* **55**, 080306 (2016).

[22] S.B. Tang, J.P. Yu, L.X. Liu, *Phys. Chem. Chem. Phys.* **15**, 5067 (2013).

[23] S. Nigam, C. Majumder, R. Pandey, *RSC Adv.* **6**, 21948 (2016).

[24] S. Nigam, S.K. Gupta, C. Majumder, R. Pandey, *Phys. Chem. Chem. Phys.* **17**, 11324 (2015).

[25] C.X. Xia, B. Xue, T.X. Wang, Y.T. Peng, Y. Jia, *Appl. Phys. Lett.* **107**, 193107 (2015).

[26] G. Kresse, J. Furthmüller, *Phys. Rev. B* **54**, 11169 (1996).

[27] J.P. Perdew, K. Burke, M. Ernzerhof, *Phys. Rev. Lett.* **77**, 3865 (1996).

[28] G. Kresse, D. Joubert, *Phys. Rev. B* **59**, 1758 (1999).

[29] S. Grimme, *J. Comput. Chem.* **27**, 1787 (2006).

[30] M. Luo, Y.E. Xu, Y.X. Song, *Optik* **144**, 334 (2017).

[31] Z. Ni, Q. Liu, K. Tang, J. Zheng, J. Zhou, R. Qin, Z. Gao, D. Yu, J. Lu, *Nano Lett.* **12**, 113 (2012).

[32] N.D. Drummond, V. Zolyomi, V.I. Falko, *Phys. Rev. B* **85**, 075423 (2012).